

Surface structures of cerium oxide nanocrystalline particles from the size dependence of the lattice parameters

S. Tsunekawa,^{a)} S. Ito, and Y. Kawazoe

Institute for Materials Research, Tohoku University, Sendai 980-8577, Japan

(Received 15 April 2004; accepted 31 August 2004)

Cerium oxide nanocrystalline particles are synthesized and monodispersed in the size range from 2 to 8 nm in diameter. The dependence of the lattice parameters on particle size is obtained by x-ray and electron diffraction analyses. The size dependence well coincides with the estimation based on the assumption that the surface is composed of one layer of Ce_2O_3 and the inside consists of CeO_2 . The effect of particle size on lattice parameters is discussed from the differences in the fabrication method and the surface structure. © 2004 American Institute of Physics. [DOI: 10.1063/1.1811771]

Cerium oxides have attracted much attention as an ultraviolet absorbent¹ for cosmetics and glass windows, and a catalyst²⁻⁴ for redox reactions in order to clean the exhaust of automobiles. The catalytic effect comes from the reversible chemical reaction between the oxygen-rich CeO_2 and the oxygen-poor Ce_2O_3 depending on the oxygen pressure.⁵ The study of surface structures of nanosize cerium oxides is expected to assist in understanding the catalysis, because it is known that the catalytic effect depends not only on the size but also on the fabrication method.

Recently, x-ray diffraction studies have shown that monodispersed cerium oxide nanocrystalline particles have a cubic fluorite-type (fcc) structure and large lattice expansions.^{6,7} This is in contrast to a decrease in the lattice parameter often observed in metal nanoparticles with decreasing particle size. Moreover, the core level shift of Ce 3d in x-ray photoelectron spectra of cerium oxide nanocrystallites has revealed that the effective valence state of Ce ions is 3.0 for a diameter of 1.4 ± 0.2 nm.⁸ The changes in the valence state and the lattice parameter are in good correlation.⁹ It is reasonable, because the decrease in cation valences necessarily results in the lattice expansion due to the increase in effective ionic radii. Very recently, electron energy loss spectroscopy has shown that for larger particles the valence reduction of cerium ions occurs mainly at the surface, forming a Ce_2O_3 layer and leaving the core as CeO_2 .¹⁰

In this letter, we estimate the thickness of the surface layer from the size dependence of the lattice parameters based on the shell and core structures and we examine the change in the lattice parameters depending on the method which was used to prepare the particles.

Figure 1 shows the size dependence of the lattice parameters, a , in our samples (cerium oxide hydrochloric acid sols) synthesized by gel-sol process and hydrothermal reaction, and monosized by ultrafiltration with a membrane and successive fractionation with a surfactant,¹¹ where D is the particle diameter obtained from electron microscopic observations. Lattice parameters were estimated by the least-squares method with a set of data, Miller indices, hkl , and lattice distances, d_{hkl} , where $d_{hkl} = (L\lambda)/r$; L is the camera length which was carefully calibrated in order to calculate exact lattice distances using the diffraction pattern of gold particles (>100 nm in diameter), λ is the electron wavelength,

0.002 51 nm at an accelerated voltage of 200 kV, and r is the radius of the diffraction ring obtained by an electron microscope (JEM-2000EX, JEOL). Figure 2 is a $\log(\Delta a) - \log(D)$ plot from the data shown in Fig. 1, where $\Delta a = a - a_0$; a_0 is the lattice parameter of the CeO_2 bulk, 0.5411 nm. The relation obtained from Fig. 2 is as follows:

$$\Delta a = 0.0324 D^{-1.04} \text{ (nm)}. \quad (1)$$

As the particles are composed of the Ce_2O_3 shell and the CeO_2 core,¹⁰ the mean lattice parameter, a_M , is obtained from the following equation, when the lattice parameter for $\text{CeO}_{1.5}$ with an average (disordered) fluorite structure¹² is represented by a_1 :

$$\begin{aligned} a &\equiv a_M = \{a_1(V_1 - V_0) + a_0V_0\}/V_1 \\ &= a_0 + 3n(a_1 - a_0)(a_1/d_1) - 3n^2(a_1 - a_0)(a_1/d_1)^2 \\ &\quad + n^3(a_1 - a_0)(a_1/d_1)^3, \end{aligned} \quad (2)$$

where $V_1 = 4\pi d_1^3/3$, $V_0 = 4\pi d_0^3/3$, and $d_1 = d_0 + na_1$; d_0 and d_1 are the radii of the core and the particle, respectively.

When $d_1 \geq 10a_1$, Eq. (2) is approximately expressed as follows:

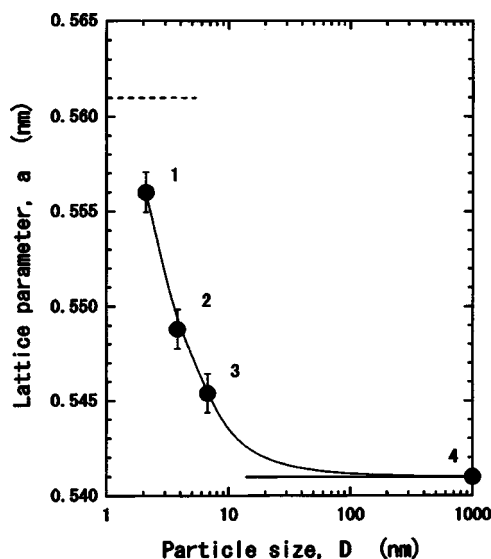


FIG. 1. Semi-log plot of fluorite-type lattice parameters as a function of the particle size. 1: 2.1 ± 0.3 nm, 2: 3.8 ± 0.6 nm, 3: 6.7 ± 0.9 nm in diameter, and 4: 99.99% CeO_2 powder. The solid line indicates the lattice parameter of the bulk CeO_2 and the dotted line a half of that of the C-type Ce_2O_3 .

^{a)}Electronic mail: scorpion@imr.edu

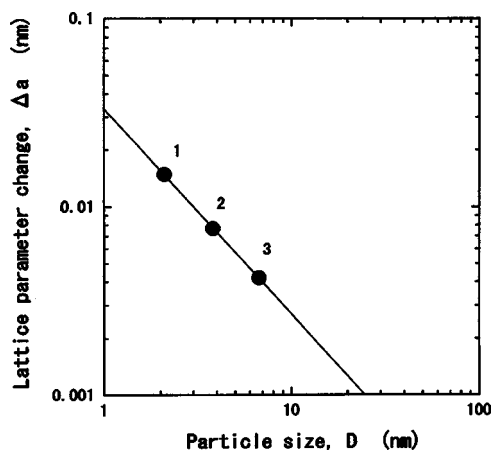


FIG. 2. Log-log plot of the change in the lattice parameter vs particle size. The numerals next to the closed circles are the same as those in Fig. 1.

$$\Delta a = a - a_0 = 3n(a_1 - a_0)a_1/d_1 = 6n(a_1 - a_0)a_1D^{-1}. \quad (3)$$

From Eqs. (1) and (3), we have the following relation:

$$6n(a_1 - a_0)a_1 \doteq 0.0324. \quad (4)$$

Considering the layer structure of Ce_2O_3 , we get $a_1 = 0.5784$ nm, $a_1 = 0.5604$ nm, $a_1 = 0.5540$ nm, and $a_1 = 0.5509$ nm using $a_0 = 0.5411$ nm, respectively, for $n = 1/4$, $n = 1/2$, $n = 3/4$, and $n = 1$. The second value is in good agreement with the lattice parameter of the average fluorite structure $\text{CeO}_{1.5}$, 0.561 nm, which is a half of that of the C-type sesquioxide Ce_2O_3 .⁶ Hence, the thickness of the Ce_2O_3 shell in the present samples should be about 0.28 nm ($=a_1/2$), if the particle diameters are more than 11 nm.

When $d_1 = a_1$, i.e., the particle is entirely composed of $\text{CeO}_{1.5}$, we have $n = 1$. For $a_1 < d_1 < 10a_1$, we have

$$1/2 < n < 1, \quad (5)$$

because the Ce 3d x-ray photoelectron spectra have shown that the increase in Ce^{3+} with decreasing particle size is monotonous.⁶ The above-mentioned results reveal that the thickness of the Ce_2O_3 shell is at most 0.561 nm, which well explain the size dependence of the lattice parameters in our samples.

Very recently, however, other size dependencies of the lattice parameters have been reported as shown in Fig. 3.^{13,14} One is made for cerium oxide nanoparticles with the diameters of 3–20 nm prepared in helium atmosphere of 1–100 Torr at about 2000 °C by a vapor phase condensation method (Wu *et al.*).¹³ The outlines of the particles are formed mostly by circular or ellipsoidal shape with few (111) surfaces. Another is obtained for monodispersed cerium oxide particles down to 6 nm in diameter synthesized by thermal decomposition of metallorganic compounds (Zhang *et al.*).¹⁴ All particles are single crystals with few stacking faults and twin boundaries and have sets of {111} planes in the high-resolution transmission electron microscopic (HRTEM) images. The order of the surface stabilization energies of unionized isolated oxygen vacancy defects on CeO_2 is $(111) < (100) < (110) < (211) < (210) < (310)$ from computer modeling calculations.^{15,16} Since the (111) surfaces is the most stable plane against the formation of surface oxygen vacancies, it is difficult to form a Ce_2O_3 layer on this type of

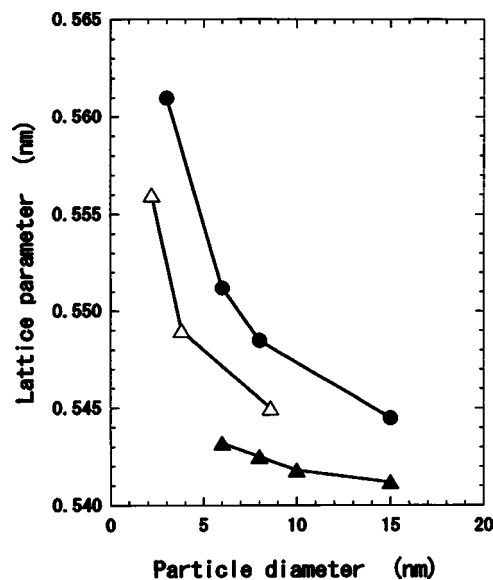


FIG. 3. Lattice parameters as a function of the particle diameter: Wu *et al.* (●), Tsunekawa *et al.* (the present result) (△), and Zhang *et al.* (▲).

surface. Applying the $\log(\Delta a) - \log(D)$ plot to the size dependence of the former (Wu *et al.*), the following relation is obtained:

$$\Delta a = 0.0600D^{-1.05} \text{ (nm)}. \quad (6)$$

By the same analysis as shown in the above discussion, we can also determine the thickness of the surface layer, t , to be $0.421 \text{ nm} \leq t \leq 0.561 \text{ nm}$ corresponding to $3/4 \leq n \leq 1$. On the other hand, the size dependence of the latter (Zhang *et al.*) is very little and does not show the relation similar to those of the present and Wu *et al.*

A typical HRTEM image for our samples is shown in Fig. 4. The particles are composed of not only octahedral but also rounded surfaces, because they are partly dissolved in strong hydrochloric acid sols.¹¹ This is known as the Berg effect,¹⁷ which acts preferentially on the edges of polygonal crystals with larger sizes on both dissolution and growth.^{18,19} Therefore, it is reasonable that the size dependence of our samples is located at the middle position in Fig. 3. When the reduction on the (111) surfaces is ignored, the fraction of rounded surfaces in our nanoparticles is approximately 67% from the thickness of the surface layers in the diameter range more than 5.6 nm, because the samples of Wu *et al.* have $n = 3/4$ and ours $n = 1/2$.

In summary, it has been concluded from the simple calculations that the present particles, which are partly dis-

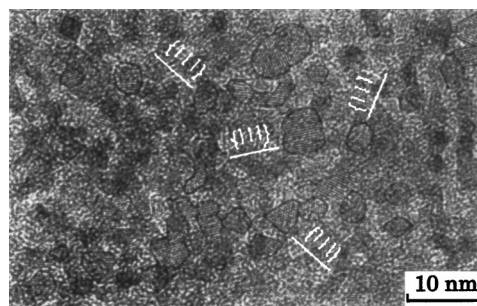


FIG. 4. (Color online) Typical HRTEM image of our samples including rounded and polygonal particles. Only the particles with clear images are illustrated by red lines.

solved in strong acid and have both rounded and octahedral boundaries, are composed of the Ce_2O_3 shell between 0.28 and 0.56 nm thick. On the other hand, the particles formed in entirely rounded and octahedral surfaces show a size dependence of the lattice parameters about two times as large as that of the present and only a little size dependence, respectively. The latter has negligible amount of Ce_2O_3 on the surfaces with the $\{111\}$ planes. It is, therefore, not expected for the particles with octahedral in shape to be a good catalyst for redox reactions.

¹S. Yabe and S. Momose, The Third Asian Cosmetic Scientist Conference, Asian Society Cosmet. Sci., Taipei, 1997, p. 103.

²J. Y. Ying and A. Tschöpe, Chem. Eng. J. **64**, 225 (1996).

³A. D. Logan and M. Shelef, J. Mater. Res. **9**, 468 (1994).

⁴H. C. Yao and Y. F. Yao, J. Catal. **86**, 254 (1984).

⁵N. V. Skorodumova, S. I. Simak, B. I. Lundqvist, I. A. Abrikosov, and B. Johansson, Phys. Rev. Lett. **89**, 166601 (2002).

⁶S. Tsunekawa, A. Kasuya, and Y. Kawazoe, Proceedings of the International Symposium on Cluster Assembled Materials, IPAP, Nagoya, 2001, p. 89.

⁷S. Tsunekawa, R. Sivamohan, S. Ito, A. Kasuya, and T. Fukuda, Nanostruct. Mater. **11**, 141 (1999).

⁸S. Tsunekawa, T. Fukuda, and A. Kasuya, Surf. Sci. **457**, L437 (2000).

⁹S. Tsunekawa, R. Sahara, Y. Kawazoe, and K. Ishikawa, Appl. Surf. Sci. **152**, 53 (1999).

¹⁰M. Suenaga (private communication); electronic mail: mas@bnl.gov.

¹¹S. Tsunekawa, R. Sivamohan, T. Ohsuna, A. Kasuya, H. Takahashi, and K. Tohji, Mater. Sci. Forum **315-317**, 439 (1999).

¹²Although the ordered structure, C-type cerium sesquioxide (bcc) the unit cell of which is two times as large as the fluorite-type one, is postulated in Ref. 7, there has been no evidence in x-ray powder diffraction patterns yet.

¹³L. Wu, H. J. Wiesmann, A. R. Moodenbaugh, R. F. Klie, Y. Zhu, D. O. Weich, and M. Suenaga, Phys. Rev. B **69**, 125415 (2004).

¹⁴F. Zhang, S.-W. Chan, J. E. Spanier, E. Apak, Q. Jin, R. D. Robinson, and I. P. Herman, Appl. Phys. Lett. **80**, 127 (2002).

¹⁵E. S. Putna, J. M. Vohs, and R. J. Gorte, J. Phys. Chem. **100**, 17862 (1996).

¹⁶J. C. Conesa, Surf. Sci. **339**, 337 (1995).

¹⁷C. W. Bunn, Discuss. Faraday Soc. **5**, 132 (1949).

¹⁸K. Onuma, K. Tsukamoto, and I. Sunagawa, J. Cryst. Growth **110**, 724 (1991).

¹⁹K. Onuma, K. Tsukamoto, and I. Sunagawa, J. Cryst. Growth **100**, 125 (1990).